

Energy Technology

Generation, Conversion, Storage, Distribution

Accepted Article

Title: Facile synthesis of carbon-coated Li₃VO₄ anode material and its application in full cells

Authors: Xueting Wang, Bin Qin, Dong Sui, Zhenhe Sun, Ying Zhou, Hongtao Zhang, and Yongsheng Chen

This manuscript has been accepted after peer review and appears as an Accepted Article online prior to editing, proofing, and formal publication of the final Version of Record (VoR). This work is currently citable by using the Digital Object Identifier (DOI) given below. The VoR will be published online in Early View as soon as possible and may be different to this Accepted Article as a result of editing. Readers should obtain the VoR from the journal website shown below when it is published to ensure accuracy of information. The authors are responsible for the content of this Accepted Article.

To be cited as: *Energy Technol.* 10.1002/ente.201800186

Link to VoR: <http://dx.doi.org/10.1002/ente.201800186>

Facile synthesis of carbon-coated Li_3VO_4 anode material and its application in full cells

Xueting Wang^[a], Bin Qin^[a], Dong Sui^[a], Zhenhe Sun^[a], Ying Zhou^[a], Hongtao Zhang^[a,b] and Yongsheng Chen^{*[a, b]}

Abstract: Li_3VO_4 is a promising anode material for lithium-ion batteries, but suffers from low electronic conductivity. Here we demonstrated a facile solid-state method to synthesize carbon-coated Li_3VO_4 (LVO/C) to enhance its electronic conductivity and electrochemical performance. The LVO/C composites exhibit preferable specific capacity, desirable cycle performance and suitable rate performance than the carbon-free Li_3VO_4 . A high reversible capacity of 456 mAh/g and 400 mAh/g can be maintained up to 100 cycles and 500 cycles at 1 C (92.2% and 80% retention of the second cycle of discharge capacity, respectively). Coupled with conventional cathodes, the fabricated full cells can deliver higher energy density than their commercial counterparts using $\text{Li}_4\text{Ti}_5\text{O}_{12}$ anodes and exhibit much more stable cycle performance than full cells using graphite anodes. The LiFePO_4 -LVO/C full cell delivers an excellent cycling stability with capacity retention of 99% vs. the second cycle after 100 cycles at 1 C. The $\text{LiNi}_{0.8}\text{Co}_{0.1}\text{Mn}_{0.1}\text{O}_2$ -LVO/C full cell delivers a maximum energy density of about 300 Wh/kg.

Introduction

Recently, rechargeable lithium-ion batteries (LIBs) have been widely used in many fields on account of its various advantages, such as high specific energy, low toxicity and long cycle life.¹ They are expected to be applied in more extensive aspects such as hybrid electric vehicles, electric vehicles and smart grids. However, the current LIBs technologies cannot perfectly satisfy the requirements in such areas due to the undesirable energy density and safety.¹⁻³ In the past few decades, graphite has been dominating the market of anode materials in rechargeable LIBs. However, graphite intercalates Li ions at a low potential close to that of Li-plating, which is a potential cause of short circuits and thus safety issues, especially at high charge-discharge rates.⁴ Great efforts have been made to search for graphite alternatives with both higher capacities and more positive intercalation voltages compared to Li/Li^+ .^{2, 4-5} $\text{Li}_4\text{Ti}_5\text{O}_{12}$ (LTO) with spinel

structure is another widely accepted insertion type anode material due to its good reversibility, zero-strain effect and safe intercalation potential (~ 1.5 V).⁶⁻⁸ However, due to its low capacity and high insertion potential, LTO anode exhibits a very low specific energy density.⁹ The alloy type anode materials, such as Si and Sn, have also been researched a lot due to their high capacities (capable of hosting 4.4 mol Li per Si or Sn). Unfortunately, they suffer from continuous capacity fading because of the huge volume change during the charge/discharge process, which hinders their practical application.^{4, 10-12} Li metal is another choice of the anode material, considering its highest theoretical capacity (3860 mAh/g) and lowest electrochemical potential. However, enormous challenges including the safety and cyclability need to be overcome before Li metal anode can enter the market.¹³⁻¹⁴

More recently, Li_3VO_4 (LVO) has been reported as a promising candidate for LIB insertion anode material with a relatively low Li insertion potential (mainly between 0.5 and 1.5 V vs. Li/Li^+) and a high capacity (with a theoretical capacity of 394 mAh/g, corresponding to $x=2$ in $\text{Li}_{3+x}\text{VO}_4$).¹² Li_3VO_4 crystallizes in the orthorhombic phase. It is built up of oxygen atoms in approximately hexagonal close packing and the cations occupy ordered tetrahedral sites.^{12, 15} According to the theoretical stimulation calculation of Li_3VO_4 crystal, the volume expansion is only $\sim 4\%$ when $x = 2$ in $\text{Li}_{3+x}\text{VO}_4$.¹⁶ Apart from all these merits, Li_3VO_4 has an intrinsic shortcoming of low electronic conductivity which may lead to large resistance polarization and poor rate capability.¹⁷⁻¹⁸ To overcome this weakness, extensive researches have been carried out to prepare the composites based on LVO, such as carbon-encapsulated Li_3VO_4 particles,¹⁹⁻²⁰ $\text{Li}_3\text{VO}_4/\text{N}$ doped C,²¹ $\text{Li}_3\text{VO}_4/\text{graphene}$,^{17, 22-23} $\text{Li}_3\text{VO}_4/\text{expanded graphite}$ ²⁴ and $\text{Li}_3\text{VO}_4/\text{carbon nanotubes (CNTs)}$.²⁵ All these studies indicate that the introduction of carbon-based materials for LVO anode materials can enhance the electronic conductivity and thus improve the electrochemical performance. However, most of the solution based methods such as sol-gel method,²⁶ hydrothermal process²⁷ and oil-bath synthesis²⁸ are complex and time-consuming, which is not facile enough for industrial application. Therefore, it is still necessary to develop a more facile route to synthesize carbon-coated Li_3VO_4 (LVO/C) composites with high performance for practical LIB applications.

Although Li_3VO_4 -based materials have been widely investigated and utilized as the anode materials in LIBs, most of their properties were only tested in the half-cell device. It is necessary to study this potential anode material in a full cell to evaluate the battery performance more accurately and is more practical.²⁹⁻³⁰ To date, there have been only a few reports about the

[a] X.T.Wang, B.Qin, D. Sui, Z. H. Sun, Y. Zhou, Dr. H.T. Zhang, Prof. Y. S. Chen
The Centre of Nanoscale Science and Technology and Key Laboratory of Functional Polymer Materials, State Key Laboratory and Institute of Elemento-Organic Chemistry, College of Chemistry, Nankai University, Tianjin, 300071, China.
E-mail: yschen99@nankai.edu.cn

[b] Dr. H.T. Zhang, Prof. Y. S. Chen
The National Institute for Advanced Materials, Nankai University, Tianjin 300071, China

Supporting information for this article is given via a link at the end of the document

performance of Li_3VO_4 composite materials as the anode paired with cathode materials of LiFePO_4 (LFP), $\text{LiNi}_{0.5}\text{Co}_{0.2}\text{Mn}_{0.3}\text{O}_2$ and $\text{LiNi}_{0.5}\text{Mn}_{1.5}\text{O}_4$ in full cells.^{15, 25, 31-32} Thus, it is important to assemble and evaluate LVO based full cells to confirm LVO's potential in lithium-ion full batteries and prove that LVO composite is an promising alternative to commercial graphite and LTO anode materials.

In this work, we demonstrated a facile solid-state synthesis method for the carbon-coated LVO (noted as LVO/C) composite. The composite exhibited significant improvements in capacity, rate capability and cycle performance compared with the controlled carbon-free LVO. The LVO/C anode material displays an initial discharge capacity of 723.6 mAh/g which is much higher than that of LVO (205.9 mAh/g) at 0.1 C (1C = 400 mA/g). After 100 cycles at 1 C, LVO/C has a high capacity of 456 mAh/g, while the pristine LVO only show a capacity of only 50 mAh/g. Furthermore, we assembled full batteries using our LVO/C composite as anode material, coupled with commercial $\text{LiNi}_{0.8}\text{Co}_{0.1}\text{Mn}_{0.1}\text{O}_2$ (NCM) and LFP as cathode materials. Then full batteries' electrochemical performance was investigated. To illustrate its practical potential, we also compared our LVO/C anode with commercial LTO and graphite anodes in full cells. As expected, LVO/C based full cells deliver higher energy density than LTO based full cells because of the higher working voltage and larger capacity of electrode materials and have better cycle stability than graphite based full cells. Our LFP-LVO/C full cell showed a pretty excellent cyclability (99% capacity retention after 100 cycles at 1 C) and NCM-LVO/C full cell delivered a maximum energy density of 300 Wh/kg, which is among the highest energy density of LVO/C full cells so far.²⁸ In general, the facile synthesis process and high electrochemical performance of LVO/C composite make it suitable for mass production and commercial applications.

Results and Discussion

Morphological and structural studies

The composites with different carbon contents were synthesized with different weight ratios of LVO and sucrose in raw materials, and the carbon content and rate performance results of these composites are shown in Table S1 and Figure S1, respectively. The optimized carbon content of 11.24% in products demonstrated the highest capacity and best cycle performance was selected for further studies. The TG-DSC curves of the optimized LVO/C composite under air flow are shown in Figure 1a. It can be seen that the only one exothermic peak is at about 415 °C in the DTA curve which corresponds to the burning of carbon in the composite.¹⁹ As shown in Figure 1b, the D-band around 1346 cm^{-1} and G-band around 1602 cm^{-1} can be seen clearly in Raman spectra of the LVO/C sample compared with the controlled carbon-free LVO, suggesting the existence of carbon in the composite. The XRD patterns of LVO and LVO/C powder are showed in Figure 1c, all diffraction peaks are sharp and can be well defined, which suggests that both of the

samples are highly crystallized. Also, both samples exhibited crystals in the pure LVO orthorhombic phase (JCPDS No. 38-1247), which is coherent with the electrochemically active LVO.⁹

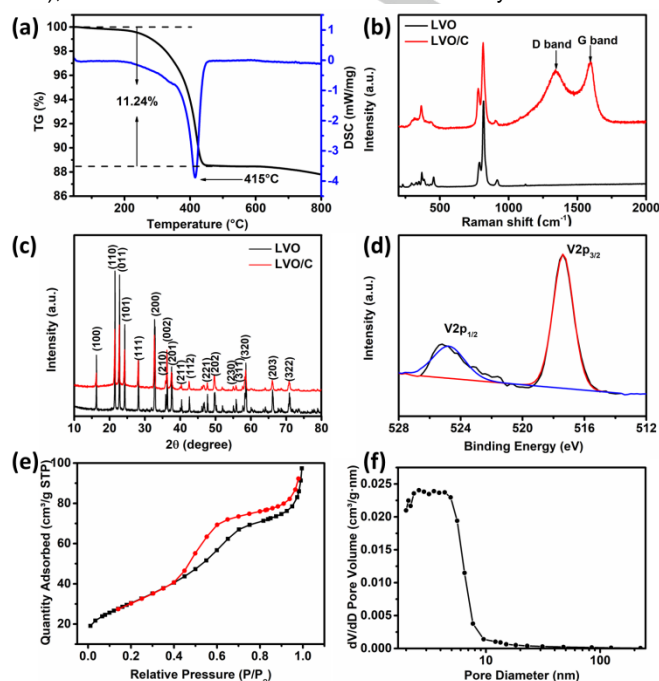


Figure 1 (a) TG-DSC curves of the LVO/C sample under air atmosphere, (b) Raman spectrum, (c) XRD pattern of the LVO and LVO/C composite and (d) V2p XPS spectra of the LVO/C composite, (e) The N_2 adsorption-desorption isotherm and (f) pore size distribution of the LVO/C.

And the carbon in the LVO/C may be amorphous since no peak attributed to crystalline carbon appears in the XRD patterns.¹⁹ Based on the XRD (111) patterns, the grain sizes were calculated to be 61.6 nm and 41.4 nm for the LVO and LVO/C samples, respectively, according to the Debye-Scherrer equation. Furthermore, the composition of the LVO/C was further characterized by XPS. The survey spectrum in Figure S2a confirms the presence of V, O, and C in the product. Figure S2b shows the high resolution spectrum of C1s, which is fitted by three peaks. The strong peak at 284.2 eV corresponds to the C=C bond, the peak at 285.8 eV can be ascribed to C-O, and the peak at near 289.8 eV can be attributed to C=O.^{21, 33-34} And as shown in Figure 1d, the high resolution spectrum of V 2p can be divided into two peaks. The peaks at 524.7 eV and 517.4 eV can be ascribed to V 2p_{1/2} and V 2p_{3/2} electrons for V in the pentavalent state.^{33, 35} This result indicates that the existence of carbon and reducing atmosphere would not reduce the pentavalent vanadium.

Nitrogen sorption isotherms were generated to investigate the Brunauer-Emmet-Teller (BET) surface and the porous structure of the samples. Figure 1e and Figure S3a are the nitrogen adsorption-desorption isotherms of LVO/C and LVO. The BET surface area and pore volume of LVO/C composite are 110 m^2/g and 0.157 cm^3/g , respectively. As expected, LVO particles

exhibit very low BET surface area ($1.31 \text{ m}^2/\text{g}$) and pore volume ($0.006 \text{ cm}^3/\text{g}$). The pore size distribution shown in Figure 1f indicates that the LVO/C composite is a mesoporous material with a narrow pore size distribution and the average pore size is 5 nm. And LVO has an average pore size of 20 nm as shown in Figure S3b. Compared to the LVO, the LVO/C composite possesses larger specific surface area and porous structure, which could offer larger contact area between electrode and electrolyte and also reduced the Li^+ ion diffusion paths.³⁶

In order to elucidate more details about the structural and morphological aspects of LVO and LVO/C powder, SEM and TEM images are exhibited in Figure 2. The SEM images in Figure 2a, b and c indicate that the carbon-free sample (LVO) holds non-uniform particles with the particle size of 3–7 μm , while particles of the carbon-coated sample (LVO/C) have much smaller size of about 200 to 500 nm. This dramatic change of morphology can be ascribed to the introduction of carbon materials in the synthesis process, which helps to restrain the particle's growth effectively.^{20, 37} Figure 2d shows the TEM images of LVO/C. The lattice spacing of 0.361 nm corresponds to the d-spacing of the (011) faces, which is consistent with the XRD pattern. In addition, an amorphous carbon layer with thickness of about 5–8 nm coating on the particles can be observed. The amorphous carbon coating layers derive from the carbonization of sucrose accompanied by the formation of LVO in the sintering process.¹⁵ Elemental mapping analysis based on energy-dispersive X-ray spectroscopy (EDX) are depicted in Figure 2e, f, g and h, from which the uniform distribution of carbon-coating layers on the LVO particles can be seen clearly.

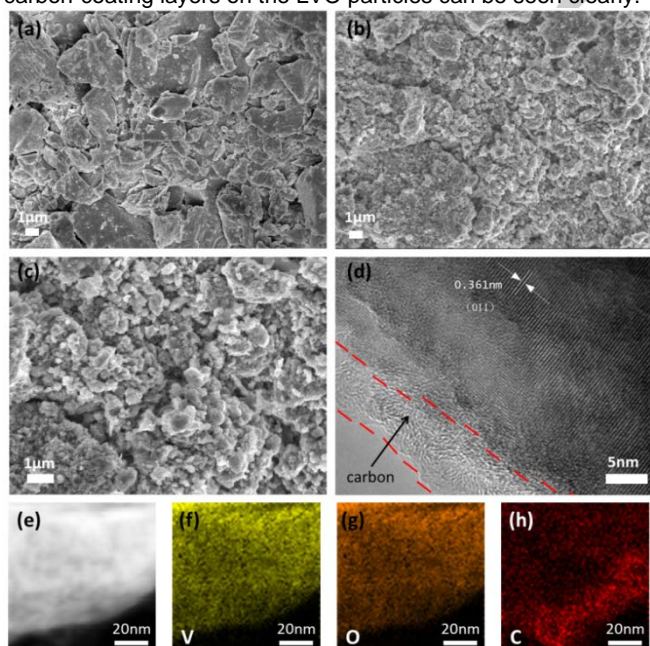


Figure 2 SEM images of the pristine LVO (a) and the LVO/C composite (b, c), TEM image of LVO/C composite (d), Elemental mapping: annual dark-field TEM image (e) and corresponding V (f), O (g) and C (h).

Electrochemical performances of LVO/C anode material in half cell devices

The half-cells with metal lithium foil as the counter electrode were used to evaluate the electrochemical performance of LVO and LVO/C as anodes for LIBs. From the charge-discharge curves in Figure 3a, it can be seen that the insertion Li^+ ions into LVO and LVO/C occurs mainly between 0.5 and 1.5 V, which means that LVO anode works at a safer voltage compared with graphite anode and a lower voltage than LTO anode. The LVO electrode displays only a discharge capacity of 205.9 mAh/g and a charge (reversible) capacity of 140.7 mAh/g at 0.1 C with an initial coulombic efficiency of 68.32% in the first cycle, while the LVO/C electrode displays a much higher discharge capacity of 723.6 mAh/g and a charge capacity of 509.9 mAh/g, corresponding to a higher initial coulombic efficiency of 70.47%. The improved capacity and coulombic efficiency can be both attributed to the carbon coating. Previous studies have proved that the LVO with bare surface is not very stable in electrolyte and would lead to side reactions at the interface including the formation of solid electrolyte interphase (SEI) film and the decomposition of the electrolyte.^{12, 19, 23, 38} Carbon is highly electrochemical insert and known for its stable SEI stability. After being coated by carbon, the active LVO-electrolyte interface turns to a more stable interface, providing a protection for the surface of LVO.^{1, 39} As for the higher capacity of the LVO/C composite, both the existence of carbon and the large surface of nano-sized particles may contribute to the high capacity via a surface or interfacial lithium

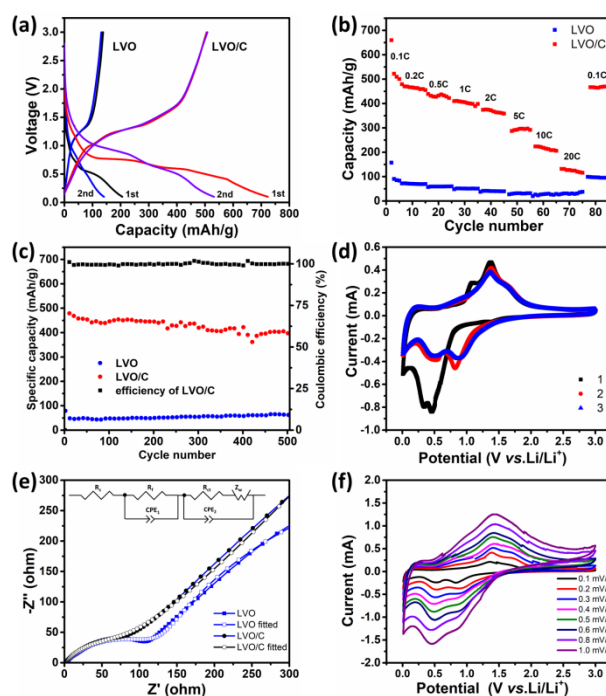


Figure 3 (a) Discharge and charge curves, (b) rate capability and (c) cycle performances. (d) CV curves of LVO/C sample between 0.1 and 3.0V, (e) EIS plot of the LVO and LVO/C electrodes, and the inset shows the equivalent circuit used to fit the plots, (f) CV curves of the LVO/C composites measured at different scan rates ranging from 0.1 to 1 mV s^{-1} .

storage mechanism.^{1,33} To illustrate the rate capability of LVO/C and LVO materials, the cells were cycled under different current densities of 0.1 ~20 C (1 C = 400 mA/g) between 0.1 and 3.0 V. Figure 3b shows the capacity retention of the LVO/C and LVO electrode at various rates. It is obvious that the LVO/C composites exhibit much improved rate performance than LVO, especially at high rates. The average discharge capacity is 500.2, 465.8, 432.2, 405.1, 371.9, 292.4, 218.3, and 126.9 mAh/g at the current rate of 0.1, 0.2, 0.5, 1, 2, 5, 10 and 20 C, respectively. After 70 cycles, the average discharge capacity can restore to 470 mAh/g when the rate reverted to 0.1 C. While for the LVO electrode, the discharge capacity is much lower (nearly 20 mAh/g) at higher rates. To explore the capacity contribution of the annealed sucrose in the composite, the half cells of the sucrose which was synthesized by the same method as the LVO/C composite was prepared. The rate performance of the annealed sucrose measured at different current densities, ranging from 0.1 C to 15 C (1 C = 400 mA/g) was shown in Figure S4a. The specific capacity of the annealed sucrose anode is 200 mAh/g at 0.1 C, and 25 mAh/g at 15 C. Details of the capacity contribution ratio of components in the composite are shown in Figure S4b. Besides the excellent rate capability of LVO/C, a high reversible capacity of 456 mAh/g and 400 mAh/g can be maintained up to 100 cycles and 500 cycles at 1 C, which is 92.2% and 80% retention of the second cycle of discharge capacity, respectively (Figure 3c). And due to the smaller surface and few defects compared with LVO/C, the capacity of LVO is better retained without obvious decay after 500 cycles at 1 C, but it has a much lower discharge capacity of only about 50 mAh/g.

Cyclic voltammetry measurements were also performed and corresponding first three cycles of the CV curves of LVO/C and LVO electrodes at a scan rate of 0.2 mV s⁻¹ between 0.1 and 3.0 V are shown in Figure 3d and Figure S5. Visible differences between the CV curves of the first and second cycle are found for both LVO and LVO/C, while the 2nd and 3rd cycles are similar. There were two reduction peaks at a voltage of 0.34 and 0.46 V in the first negative scan, which corresponds to the insertion of Li-ion into the LVO/C and the formation of SEI.^{19,27,31,40} The two reduction peaks shifted to 0.48 and 0.83 V in the subsequent scans, which can be ascribed to the activation of the LVO/C electrode.^{19,27,35} The profiles for the first three anodic scans are similar, displaying a main broad oxidation peak near 1.37 V, which is attributed to the extraction of Li-ion from the Li_{3+x}VO₄.^{19,27,40} Figure 3e shows the Nyquist plots of the LVO and LVO/C after 10 cycles at 0.1 C to further investigate the charge-transport kinetics for both samples. The EIS spectra show a compressed semicircle and a line inclined at about 45° at the low frequency. The intercept in high frequency can be ascribed to ohmic resistance caused by electrolyte (*R*_s) and/or SEI film (*R*_i), the medium-frequency semicircle is due to the charge-transfer impedance on electrode/electrolyte interface (*R*_{ct}), and the inclined line in low-frequency corresponds to the Li-ion diffusion process within electrodes.²⁰⁻²¹ The values of *R*_{ct} for the LVO and LVO/C electrodes were calculated to be 134.3 and 86.4 Ω, respectively, indicating that the LVO/C composite

has faster charge transfer. CV curves of both samples were also measured at different scan rates from 0.1 to 1.0 mV/s (Figure 3f and Figure S7). There is a good linear relationship between the oxidation peak current (*I*_{pa}) and the square root of the scan rate (*v*^{1/2}) (Figure S6), suggesting a diffusion-controlled process in the charge and discharge process.^{15,36,41} Thus the Li⁺ diffusion is a key factor to the electrode kinetics.⁴² Accordingly, the apparent Li⁺ ion diffusion coefficient can be calculated based on the Randles-Sevcik equation (eq 1)^{20,36}:

$$I_{pa} = 0.4463nFC_{Li^+}A\sqrt{\frac{nFvD}{RT}} \quad (1)$$

Where *n* is the number of electrons involved in the reaction of the redox couple, *F* is Faraday's constant, *C*_{Li⁺} is the concentration of Li⁺ ions, *A* is the working electrode area, *v* is the scan rate, *R* is the gas constant, and *T* is the absolute temperature.³⁶ According to the slope of the fitting line (Figure S6), the apparent Li⁺ ion diffusion coefficient of LVO/C is calculated to be 2.83×10⁻⁹ cm² s⁻¹, which is much higher than that of LVO (2.55 × 10⁻¹¹ cm² s⁻¹, calculated from Figure S7b). The higher apparent Li⁺ ion diffusion coefficient should be attributed to the smaller particle size and carbon coating of LVO/C composites, which are favorable for Li⁺ ion diffusion. And this is in accordance with the previous studies which have revealed that smaller particle size of the electrode materials could provide a large surface for Li⁺ flux and shorter Li⁺ ion diffusion path lengths and thus lead to a high reactivity.^{43,44} Besides, smaller particle size of electrode materials is also beneficial for good inhibition of the lithium insertion/extraction strain and the improvement of recharge ability of the battery materials.^{1,43,45} These results show that the LVO/C has a smaller charge transfer resistance and higher apparent Li⁺ ion diffusion coefficient, which permits fast electron and Li⁺ ions transports and obtain good performance. The carbon-coating layers not only restrain the particle's growth but also enhance the electrical interconnection between the LVO particles.

Performance of full cell devices

The electrochemical performances of LVO/C composite were also investigated in the full cell versus the commercial LFP and NCM. In the initial 100 cycles, the LFP-LVO/C batteries showed an excellent cycling performance with capacity retention of 99% (vs. the 2nd cycle), accompanying a working voltage of around 2.4 V (Figure 4a). For this LFP-LVO/C full cell, the Coulombic efficiency in the first cycle was 68% (i.e., a discharge capacity of 387 mAh g_{anode}⁻¹ and a charge capacity of 565.7 mAh g_{anode}⁻¹ at 0.1 C), and it increased quickly to 95% in the second cycles. Within subsequent several cycles, the Coulombic efficiency reached close to 100% and maintained stable (Figure 4b). The reason for the low Coulombic efficiency of the full cell in the first cycle may be the decomposition of electrolyte and the formation of a solid-electrolyte interface.^{29,46} Figure S8 compares the EIS plots of the LFP-LVO/C full cell before and after the cycle test. As can be seen in Figure 4c, at rate of 0.1 C (1 C = 400 mA/g), 0.2 C, 0.5 C, 1 C, 2 C, 5 C, 10 C and 15 C, the cell could still

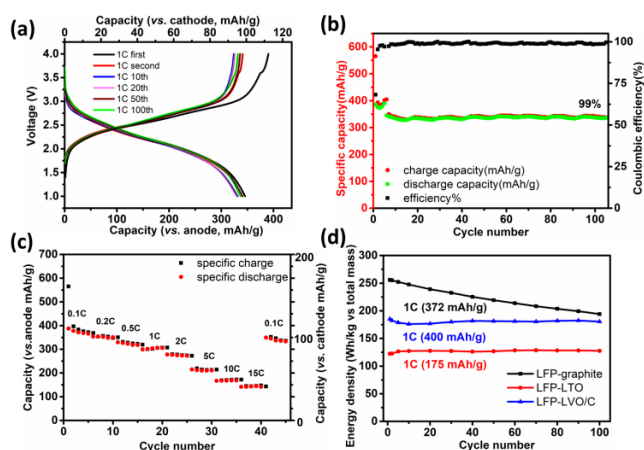


Figure 4 (a) Charge-discharge and (b) cycling ability curves in the initial 100 cycles at 1 C (1 C = 400 mA g⁻¹), (c) rate capability under different rate from 0.1 C to 15 C of LFP-LVO/C full cell, (d) energy density comparison of LFP-LVO/C with LFP-LTO and LFP-graphite.

work well with capacities of 387.4, 353.5, 329.9, 299.5, 278.1, 215.4, 167.2 and 141.9 mAh g_{anode}⁻¹, respectively. Finally, the capacity of the cell could recover back to 349.7 mAh g_{anode}⁻¹ at the rate of 0.1 C, demonstrating the good rate capability and stability of the electrode material. Furthermore, the energy density comparison of LFP-LVO/C and LFP-LTO, LFP-graphite full cells was made to illustrate the practical application potential for LVO/C composite. The energy densities were calculated by the following equation (eq 2)⁴⁷:

$$\text{energy density} = \frac{C_C \times C_A}{C_C + C_A} \times V_{op} \quad (2)$$

where C_C , C_A , and V_{op} are cathode capacity, anode capacity, and operation voltage respectively. As can be seen in Figure 4d, at the beginning of the cycle, the energy density of LFP-graphite is much higher than that of LFP-LVO/C, since the graphite has a much lower charge-discharge voltage and thus a wider voltage window (about 3.2 V). After 100 cycles at 1 C (for LFP-graphite 1 C = 372 mA g⁻¹, for LFP-LTO 1 C = 175 mA g⁻¹), the energy density of LFP-LVO/C (180.6 Wh kg_{total mass}⁻¹) is approaching to that of LFP-graphite (194.2 Wh kg_{total mass}⁻¹), and they are both higher than that of LFP-LTO (127.7 Wh kg_{total mass}⁻¹). The full cell composed of LVO/C anode material has a better cyclability and is safer than graphite anode material. At the same time, it also has a higher energy density than LTO, which indicates that LVO/C anode has the potential to practical application by combining the strengths of LTO and graphite anodes. Furthermore, the full cells with the cathode material of NCM were also investigated to verify the practicability of LVO/C composite. It is noteworthy that the NCM-LVO/C full cell exhibits a maximum energy density of 300 Wh kg_{total mass}⁻¹ at 0.1 C due to the larger capacity and higher working voltage of NCM than that of LFP (as shown in Figure S10). The NCM-LVO/C full cell delivered an energy density of 265 Wh kg_{total mass}⁻¹ at 1 C and

showed a capacity retention of 86.5% (vs. the 2nd cycle) after 100 cycles, accompanying a working voltage of around 2.9 V.

Conclusions

A facile solid-state preparation method for the LVO and LVO/C composite as the LIBs anode material was developed. The prepared LVO/C composite showed better rate capacity and cycle performance than pristine LVO due to the higher lithium diffusion coefficient and electronic conductivity by simple carbon coating. The LVO/C material displays an initial discharge capacity of 723.6 mAh/g, a good rate capability of 126.9 mAh/g at 20 C and a decent cycle stability with a reversible capacity of 456 mAh/g and 400 mAh/g after 100 cycles and 500 cycles at 1 C (92.2% and 80% retention of the second of discharge capacity), respectively. Furthermore, the full cell based on LVO/C (LFP-LVO/C and NCM-LVO/C) were fabricated and investigated. After 100 cycles at 1 C, the LFP-LVO/C cell could deliver an energy density of 180.6 Wh kg_{total mass}⁻¹, which is comparable to the LFP-graphite full cell (194.2 Wh kg_{total mass}⁻¹) and much higher than that of LFP-LTO full cell (127.7 Wh kg_{total mass}⁻¹). LFP-LVO/C full cell also shows excellent cyclability (99%), which is similar to that of LFP-LTO full cell (~100%). Moreover, NCM-LVO/C batteries exhibited a maximum energy density of 300 Wh kg_{total mass}⁻¹. The above results indicate the LVO/C anode material prepared by our facile solid-state reaction method has high energy density, good cyclability and desirable safety. Therefore, it is a potential anode material for mass production and further practical application.

Experimental Section

Materials synthesis: LVO and LVO/C were prepared by a solid-state reaction method. All the raw materials were commercial obtained. Typically, stoichiometric amounts of dried V₂O₅ and Li₂CO₃ (Li:V=3:1 in molmol⁻¹), and sucrose (different weight ratio with theoretical yield of LVO) were mixed in water were commercial obtained. The solution was stirred overnight and wet ball milled (by Mini Zeta at 30.00 Hz, 1800 r/min) for 4 h followed by desiccation. Finally, the mixture powders were pressed into tablets before sintered at 300 °C for 5 h and 750 °C for 8 h under a H₂/Ar (5:95 v/v) atmosphere to get the final product. For comparison, carbon-free LVO (without adding glucose) was also prepared using the same route.

Characterization: Thermogravimetric (TG) measurements (TGA/SDTA 851^e) were conducted from room temperature to 800 °C at a heating rate of 10 °C min⁻¹ in air. The surface morphology was characterized by SEM (JEOL, JSM-7500F) with acceleration voltage of 5 kV. The transmission electron microscopy (TEM) investigation was performed on a Philips Technical G2 F20 instrument at 200 kV. Power X-ray diffractometer (XRD) analysis was performed on an Ultrama IV, Rigaku diffractometer with Cu K α radiation (data were collected from powder samples at a scanning rate of 20 degree min⁻¹ for 2 θ in the range of 10–80°). X-ray photoelectron spectroscopy (XPS) was carried out using AXIS HIS 165 spectrometer (Kratos Analytical) with a monochromatized Al K α X-ray source (1486.71 eV photons) to analyze the chemical composition of the products.

Cell fabrication and electrochemical characterization:

Electrochemical measurements were carried out using coin-type cells (CR2430). The electrodes films were prepared by mixing the as-synthesized sample or commercial cathodes (LFP, Tianjin STL ENERGY TECHNOLOGY CO., LTD.; NCM, Tianjin PlanNano) with conducting agent (super P) and polyvinylidene fluoride binder (PVDF, in N-methyl-2-pyrrolidone) with a weight ratio of 8:1:1 in an agate mortar. The obtained homogeneous slurry was coated on a 10 μm thick Cu foil (anode) or Al foil (cathode) uniformly. After heating at 60 $^{\circ}\text{C}$ for 3h in air-circulating oven and 150 $^{\circ}\text{C}$ for 1h under vacuum, the electrode sheet was pressed and punched into ~ 12 mm diameter electrodes with a mass loading of 1-2 mg cm^{-2} . And then the electrodes were dried at 180 $^{\circ}\text{C}$ for 6 h before the coin-type cells were assembled in an argon-filled glove box. For half lithium ion batteries, lithium metal foils were used as counter electrodes and the specific capacity was based on the active material in the composite electrode and for full cells, the cathodes were LFP or NCM. The full cells were designed with an N/P ratio of ~ 1.1 , the loading values of the active materials for cathode materials were 1-4.5 mg cm^{-2} . And the electrolyte was 1M LiPF_6 in ethylene carbonate (EC): dimethyl carbonate (DMC): diethyl carbonate (DEC) (1:1:1 vol. %). Clegard 2325 (PP/PE/PP 25 μm) was used as the separator. The electrochemical performances were measured with two-electrode electrochemical cell by an automatic battery tester system (Land CT2001A model, Wuhan LAND electronics Co., Ltd.) at room temperature. For the high current density cycle performance, the electrode was pretreated after conditional cycling, that is to say, the electrode, which was intended to cycle under 1 C (1 C = 400 mA/g, would be previously cycled after five charge-discharge cycles at rate of 0.1 C). Cyclic voltammetry (CV) and electrochemical impedance spectroscopy (EIS) were collected on Autolab system (Metrohm). The CV curves were recorded at various scanning rates from 0.1 mV/s to 1 mV/s at potential ranges of 0.1-3.0 V, and the impedance spectra were recorded by applying an AC voltage of 5 mV in the frequency range from 1 MHz to 0.01 Hz.

Acknowledgements

The authors gratefully acknowledge financial support from the Ministry of Science and Technology of China (MoST, 2016YFA0200200), the National Natural Science Foundation of China (NSFC, 21421001, 51633002, and 51472124), Tianjin city (16ZXCLGX00100) and 111 Project (#B12015).

Keywords: solid-state reaction, carbon-coated Li_3VO_4 , anode material, full cell

- [1] Liao, C.; Zhang, Q.; Zhai, T.; Li, H.; Zhou, H. *Energy Storage Mater.* **2017**, *7*, 17-31.
- [2] Liang, Z. Y.; Zhao, Y. M.; Dong, Y. Z.; Kuang, Q.; Lin, X. H.; Liu, X. D.; Yan, D. L. *J. Electroanal. Chem.* **2015**, *745*, 1-7.
- [3] Goodenough, J. B.; Park, K. S. *J. Am. Chem. Soc.* **2013**, *135*, 1167-1176.
- [4] Manthiram, A. *J. Phys. Chem. Lett.* **2011**, *2*, 176-184.
- [5] Kim, M. G.; Cho, J. *Adv. Funct. Mater.* **2009**, *19*, 1497-1514.
- [6] Aravindan, V.; Lee, Y. S.; Madhavi, S. *Adv. Energy Mater.* **2015**, *5*, 1402225.
- [7] Yi, T.-F.; Yang, S.-Y.; Xie, Y. *J. Mater. Chem. A* **2015**, *3*, 5750-5777.
- [8] Liu, C.; Wang, S.; Zhang, C.; Fu, H.; Nan, X.; Yang, Y.; Cao, G. *Energy Storage Mater.* **2016**, *5*, 93-102.
- [9] Tartaj, P.; Amarilla, J. M.; Vazquez-Santos, M. B. *Chem. Mater.* **2016**, *28*, 986-993.
- [10] Park, C. M.; Kim, J. H.; Kim, H.; Sohn, H. J. *Chem. Soc. Rev.* **2010**, *39*, 3115-3141.
- [11] Chan, C. K.; Peng, H.; Liu, G.; McIlwrath, K.; Zhang, X. F.; Huggins, R. A.; Cui, Y. *Nat. Nanotechnol.* **2008**, *3*, 31-35.
- [12] Li, H. Q.; Liu, X. Z.; Zhai, T. Y.; Li, D.; Zhou, H. S. *Adv. Energy Mater.* **2013**, *3*, 428-432.
- [13] Lin, D.; Liu, Y.; Cui, Y. *Nat. Nanotechnol.* **2017**, *12*, 194-206.
- [14] Xu, W.; Wang, J.; Ding, F.; Chen, X.; Nasybulin, E.; Zhang, Y.; Zhang, J.-G. *Energy Environ. Sci.* **2014**, *7*, 513-537.
- [15] Yang, Y.; Li, J. Q.; Chen, D. Q.; Zhao, J. B. *J. Electrochem. Soc.* **2017**, *164*, A6001-A6006.
- [16] Arroyo-de Dompablo, M. E.; Tartaj, P.; Amarilla, J. M.; Amador, U. *Chem. Mater.* **2016**, *28*, 5643-5651.
- [17] Shi, Y.; Wang, J. Z.; Chou, S. L.; Wexler, D.; Li, H. J.; Ozawa, K.; Liu, H. K.; Wu, Y. P. *Nano Lett.* **2013**, *13*, 4715-4720.
- [18] Zhang, C. K.; Wang, K.; Liu, C. F.; Nan, X. H.; Fu, H. Y.; Ma, W. D.; Li, Z. Y.; Cao, G. Z. *NPG Asia Mater.* **2016**, *8*, e287.
- [19] Liang, Z. Y.; Lin, Z. P.; Zhao, Y. M.; Dong, Y. Z.; Kuang, Q.; Lin, X. H.; Liu, X. D.; Yan, D. L. *J. Power Sources* **2015**, *274*, 345-354.
- [20] Zhang, C.; Song, H.; Liu, C.; Liu, Y.; Zhang, C.; Nan, X.; Cao, G. *Adv. Funct. Mater.* **2015**, *25*, 3497-3504.
- [21] Zhang, J. C.; Ni, S. B.; Ma, J. J.; Yang, X. L.; Zhang, L. L. *J. Power Sources* **2016**, *301*, 41-46.
- [22] Liu, J.; Lu, P. J.; Liang, S.; Liu, J.; Wang, W.; Lei, M.; Tang, S.; Yang, Q. *Nano Energy* **2015**, *12*, 709-724.
- [23] Jian, Z.; Zheng, M.; Liang, Y.; Zhang, X.; Gheyhani, S.; Lan, Y.; Shi, Y.; Yao, Y. *Chem. Commun.* **2015**, *51*, 229-231.
- [24] Hu, S.; Song, Y. F.; Yuan, S. Y.; Liu, H. M.; Xu, Q. J.; Wang, Y. G.; Wang, C. X.; Xia, Y. Y. *J. Power Sources* **2016**, *303*, 333-339.
- [25] Li, Q.; Sheng, J.; Wei, Q.; An, Q.; Wei, X.; Zhang, P.; Mai, L. *Nanoscale* **2014**, *6*, 11072-11077.
- [26] Du, C. Q.; Wu, J. W.; Liu, J.; Yang, M.; Xu, Q.; Tang, Z. Y.; Zhang, X. H. *Electrochim. Acta.* **2015**, *152*, 473-479.
- [27] Ni, S. B.; Lv, X. H.; Ma, J. J.; Yang, X. L.; Zhang, L. L. *J. Power Sources* **2014**, *248*, 122-129.
- [28] Li, Q.; Wei, Q.; Wang, Q.; Luo, W.; An, Q.; Xu, Y.; Niu, C.; Tang, C.; Mai, L. *J. Mater. Chem. A* **2015**, *3*, 18839-18842.
- [29] Ming, H.; Ming, J.; Oh, S.-M.; Lee, E.-J.; Huang, H.; Zhou, Q.; Zheng, J.; Sun, Y.-K. *J. Mater. Chem. A* **2014**, *2*, 18938-18945.
- [30] Hai, M.; Jun, M.; Jingyi, Q.; Zhongbao, Y.; Meng, L.; Zheng, J. *Prog. Chem.* **2016**, *28*, 204-218.
- [31] Zhang, J. C.; Ni, S. B.; Kang, T.; Tang, J.; Yang, X. L.; Zhang, L. L. *J. Mater. Chem. A* **2016**, *4*, 14101-14105.
- [32] Shen, L.; Chen, S.; Maier, J.; Yu, Y. *Adv. Mater.* **2017**, 1701571.
- [33] Zhang, C.; Liu, C.; Nan, X.; Song, H.; Liu, Y.; Zhang, C.; Cao, G. *ACS Appl. Mater. Interfaces* **2016**, *8*, 680-688.
- [34] Cai, Z.; Xu, L.; Yan, M.; Han, C.; He, L.; Hercule, K. M.; Niu, C.; Yuan, Z.; Xu, W.; Qu, L.; Zhao, K.; Mai, L. *Nano Lett.* **2015**, *15*, 738-744.
- [35] Liang, Z. Y.; Zhao, Y. M.; Ouyang, L. Z.; Dong, Y. Z.; Kuang, Q.; Lin, X. H.; Liu, X. D.; Yan, D. L. *J. Power Sources* **2014**, *252*, 244-247.
- [36] Yang, Y.; Li, J. Q.; He, X. Y.; Wang, J.; Sun, D.; Zhao, J. B. *J. Mater. Chem. A* **2016**, *4*, 7165-7168.
- [37] Li, H.; Zhou, H. *Chem. Commun.* **2012**, *48*, 1201-1217.
- [38] He, C.; Wu, S.; Zhao, N.; Shi, C.; Liu, E.; Li, J. *ACS Nano* **2013**, *7*, 4459-4469.
- [39] Pohjalainen, E.; Kallioinen, J.; Kallio, T. *J. Power Sources* **2015**, *279*, 481-486.
- [40] Kim, W. T.; Jeong, Y. U.; Lee, Y. J.; Kim, Y. J.; Song, J. H. *J. Power Sources* **2013**, *244*, 557-560.
- [41] Ni, S. B.; Zhang, J. C.; Lv, X. H.; Yang, X. L.; Zhang, L. L. *J. Power Sources* **2015**, *291*, 95-101.
- [42] Mi, Y. Y.; Gao, P.; Liu, W.; Zhang, W. D.; Zhou, H. H. *J. Power Sources* **2014**, *267*, 459-468.

- [43] Zhang, Q.; Uchaker, E.; Candelaria, S. L.; Cao, G. *Chem. Soc. Rev.* **2013**, *42*, 3127-3171.
- [44] Zhang, J. J.; Yu, A. S. *Sci. Bull.* **2015**, *60*, 823-838.
- [45] Qin, R.; Shao, G.; Hou, J.; Zheng, Z.; Zhai, T.; Li, H. *Sci. Bull.* **2017**, *62*, 1081-1088.
- [46] Jung, H. G.; Jang, M. W.; Hassoun, J.; Sun, Y. K.; Scrosati, B. *Nat. Commun.* **2011**, *2*, 516.
- [47] Zhang, X.; Qiu, X.; Kong, D.; Zhou, L.; Li, Z.; Li, X.; Zhi, L. *ACS Nano* **2017**, *11*, 7476-7484.

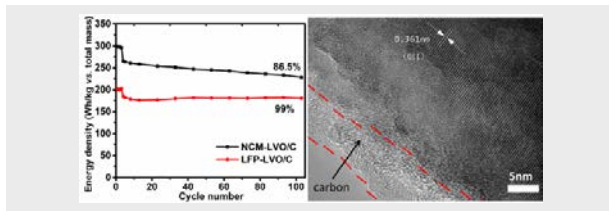
WILEY-VCH

Accepted Manuscript

Entry for the Table of Contents (Please choose one layout)

Layout 2:

FULL PAPER



Xueting Wang^[a], Bin Qin^[a], Dong Su^[a],
Zhenhe Sun^[a], Ying Zhou^[a], Hongtao
Zhang^[a, b] and Yongsheng Chen^{*[a, b]}

**Facile synthesis of carbon-coated
Li₃VO₄ anode material and its
application in full cells**

Li₃VO₄ is a promising lithium-ion batteries anode material, but suffers from low electronic conductivity. We demonstrated a facile solid-state method to synthesis carbon-coated Li₃VO₄ (LVO/C). A high reversible capacity of 400 mAh/g can be maintained up to 500 cycles at 1 C. Paired with conventional cathodes, the fabricated full cells deliver a maximum energy density of about 300 Wh/kg.

Accepted Manuscript